

A DOUBLE NEUTRON STAR MERGER ORIGIN FOR THE COSMOLOGICAL RELATIVISTIC FADING SOURCE PTF11AGG?

XUE-FENG WU^{1,2,*}, HE GAO^{1,3}, XUAN DING¹, BING ZHANG^{3,4,5}, ZI-GAO DAI⁶, JIAN-YAN WEI⁷

¹Purple Mountain Observatory, Chinese Academy of Sciences, Nanjing, 210008, China; xfwu@pmo.ac.cn

²Chinese Center for Antarctic Astronomy, Chinese Academy of Sciences, Nanjing, 210008, China

³Department of Physics and Astronomy, University of Nevada Las Vegas, NV 89154, USA

⁴Department of Astronomy, Peking University, Beijing 100871, China

⁵Kavli Institute of Astronomy and Astrophysics, Peking University, Beijing 100871, China

⁶School of Astronomy and Space Science, Nanjing University, Nanjing 210093, China

⁷National Astronomical Observatories, Chinese Academy of Sciences, Beijing 100012, China

Draft version June 20, 2018

ABSTRACT

The Palomar Transient Factory (PTF) team recently reported the discovery of a rapidly fading optical transient source, PTF11agg. A long-lived scintillating radio counterpart was identified, but the search for a high energy counterpart showed negative results. The PTF team speculated that PTF11agg may represent a new class of relativistic outbursts. Here we suggest that a neutron star (NS)-NS merger system with a supra-massive magnetar central engine could be a possible source to power such a transient, if our line of sight is not on the jet axis direction of the system. These systems are also top candidates for gravitational wave sources to be detected in the advanced LIGO/Virgo era. We find that the PTF11agg data could be explained well with such a model, suggesting that at least some gravitational wave bursts due to NS-NS mergers may be associated with such a bright electromagnetic counterpart without a γ -ray trigger.

Subject headings: gravitational waves, radiation mechanisms: non-thermal, stars: neutron

1. INTRODUCTION

Recently, Cenko et al. (2013) (hereafter C13) reported a new discovery from the Palomar Transient Factory (PTF), named as PTF11agg. A multi-wavelength counterpart search was performed for this rapidly fading optical transient. While a year-long scintillating radio counterpart was identified, no high energy counterpart was found. Based on a late-time, deep optical observation which revealed a faint, quiescent source at the transient location, C13 suggested a cosmological origin for this transient. If so, a relativistic ejecta is required in order to explain the incoherent radio emission.

Many cosmological sources have been known (or proposed) to be able to generate relativistic ejecta, such as active galactic nuclei (Ghisellini et al. 1993; Krawczynski & Treister 2013), gamma-ray bursts (GRBs; Zhang & Mészáros 2004; Mészáros 2006; Gehrels & Razzaque 2013), tidal disruption of a star by a supermassive black hole (Burrows et al. 2011; Bloom et al. 2011; Cenko et al. 2012; Lei & Zhang 2011; Lei et al. 2013), as well as core-collapse supernova without GRB association (Soderberg et al. 2010). Among these sources, the GRB afterglows have the most similar observed properties to PTF11agg, regardless of the fact that PTF11agg has no high energy counterparts. If PTF11agg is indeed a GRB afterglow, the lack of a high energy signature could be explained in two ways: an on-axis burst but without a high energy band trigger due to a lack of satellite coverage; or an off-axis burst that gives rise to an “orphan” afterglow emerging due to a viewing-angle effect (Rhoads 1997; Nakar et al. 2002). C13 considered both possibilities: it turns out the likelihood of an “untriggered” on-axis long GRB being discovered by PTF is quite small (2.6%), and the off-axis afterglow model fails to interpret both the optical and radio data. They therefore speculated that PTF11agg may represent a new class of relativistic outburst.

Numerical simulations show that binary neutron star (NS) mergers would launch a mildly anisotropic outflow during the merger process, which has a typical mass of about $10^{-4} \sim 10^{-2} M_{\odot}$ and a typical velocity of about $0.1 - 0.3c$ (where c is the speed of light) (e.g. Rezzolla et al. 2011; Rosswog et al. 2013; Hotokezaka et al. 2013). Moreover, if the equation of state of nuclear matter is stiff as supported by the current data, a stable supra-massive magnetar would form after the merger (Dai et al. 2006; Zhang 2013; Giacomazzo & Perna 2013). If so, the proto-magnetar would eject a near-isotropic Poynting flux dominated outflow. Similar to the GRB pulsar energy injection model (Dai & Lu 1998a,b; Zhang & Mészáros 2001), the magnetar would accelerate the ejecta to a mildly or even highly relativistic speed, producing a strong external shock upon interaction with the ambient medium to give rise to strong broad-band emission (Gao et al. 2013a). Hereafter, we define such a model as the “double neutron star (DNS) merger” afterglow model. Such an afterglow signal is similar to GRBs, which can naturally explain the lack of a high-energy counterpart. We suggest that PTF11agg might be the first recognized detection of MDNSM afterglow emission.

2. OBSERVATIONS OF PTF11AGG

PTF11agg was first detected by the Palomar 48 inch Oschin telescope at 5:17:11 on 2011 January 30, and is located at R.A.(J2000.0) = $08^{\text{h}}22^{\text{m}}17.195^{\text{s}}$, decl.(J2000.0) = $+21^{\circ}37'38''.26$. In the R band, the source shows decay behavior from the very beginning, with $R = 18.26 \pm 0.05$ mag in the first detection image and a faint last detection $R = 22.15 \pm 0.33$ mag on 2011 February 1. Checking back to 2009 November, no optical emission was reported at this location. Late-time ($\Delta t > 1$ month) deep optical observation revealed a faint, unresolved source in g' and R bands at R.A.(J2000.0) = $08^{\text{h}}22^{\text{m}}17.202^{\text{s}}$, decl.(J2000.0) = $+21^{\circ}37'38''.26$. Based on this detection, C13 speculated that the redshift of PTF11agg

should fall somewhere in the range $0.5 \lesssim z \lesssim 3.0$. The R band light curve of PTF11agg could be fitted well by a power-law with a best-fit index $\alpha = 1.66 \pm 0.35$, if $t_0 = 23:34$ UT (± 1.7 hr) on 2011 January 29 is taken as the onset time.

Besides optical observation, the Karl G. Jansky Very Large Array (Perley et al. 2011) was also employed to observe the radio counterpart of PTF11agg, starting from 2011 March 11, with a total bandwidth 8 GHz and local oscillator frequency 93.6 GHz. The spectral energy distribution in the radio band was constructed at two epochs on 2011 March 14 and 2011 April 7, and both can be fitted with a power law with an index $\beta = 1/3$ (convention $F_\nu \propto \nu^\beta$). Based on the constraints from the angular diameter of the emitting region, C13 inferred that PTF11agg was initially at least modestly relativistic.

C13 also checked the archival data from three primary high-energy facilities for GRB triggers, i.e. InterPlanetary Network (Hurley et al. 2010), the Gamma-ray Burst Monitor on the *Fermi* spacecraft (Meegan et al. 2009), and Burst Alert Telescope on the *Swift* spacecraft (Barthelmy et al. 2005)). No temporally coincident triggers were reported in the direction of PTF11agg. The X-Ray Telescope (Burrows et al. 2005) on *Swift* was also later employed to observe the location of PTF11agg on 2011 March 13, but no X-ray source was detected.

3. DNS MERGER AFTERGLOW MODEL AND APPLICATION TO PTF11AGG

Gao et al. (2013a) recently proposed that the DNS merger scenario with a supra-massive magnetar central engine could power bright, broad-band electromagnetic signals, behaving similarly to GRB afterglow emission. The basic picture of such a scenario is the following:

A stable supra-massive magnetar has a total spin energy $E_{\text{rot}} = (1/2)I\Omega_0^2 \simeq 2 \times 10^{52} I_{45} P_{0,-3}^2$ erg (with $I_{45} \sim 1.5$ for a massive NS), where P_0 is the initial spin period of the magnetar. Throughout this letter, we use the convention $Q = 10^n Q_n$ in cgs units, except ejecta mass M_{ej} , which is in units of solar mass M_\odot . The spindown luminosity and the characteristic spindown time scale critically depend on the dipole magnetic field strength B_p and initial spin period P_0 (which may be close to the break-up limit), i.e. $L_{\text{sd}} = L_{\text{sd},0}/(1+t/t_{\text{sd}})^2$, where $L_{\text{sd},0} \simeq 10^{49}$ erg s $^{-1}$ $B_{p,15}^2 R_6^6 P_{0,-3}^4$, and $t_{\text{sd}} \simeq 2 \times 10^3$ s $I_{45} B_{p,15}^{-2} P_{0,-3}^2 R_6^{-6}$, where $R = 10^6 R_6$ cm is the stellar radius. The dynamics of the blastwave is defined by energy conservation (Gao et al. 2013a)

$$L_0 t = (\gamma - 1) M_{\text{ej}} c^2 + (\gamma^2 - 1) M_{\text{sw}} c^2, \quad (1)$$

where $L_0 = \xi L_{\text{sd},0}$ is the magnetar injection luminosity into the blastwave, and $M_{\text{sw}} = (4\pi/3) R^3 n m_p$ is the swept-up mass from the interstellar medium.

Initially, one has $(\gamma - 1) M_{\text{ej}} c^2 \gg (\gamma^2 - 1) M_{\text{sw}} c^2$, so that the kinetic energy of the ejecta would increase linearly with time until $t = \min(t_{\text{sd}}, t_{\text{dec}})$, where the deceleration time t_{dec} is defined by the condition $(\gamma - 1) M_{\text{ej}} c^2 = (\gamma^2 - 1) M_{\text{sw}} c^2$. After t_{dec} , the blastwave enters a self-similar phase described by the Blandford-McKee self-similar solution (Blandford & McKee 1976). In this phase, the dynamics of the blastwave is only determined by a few parameters (e.g. the total energy of the system and the ambient density).

During all of the dynamical phases for the ejecta, a strong external shock would be formed upon interaction with the ambient medium, where particles are believed to be accelerated, giving rise to broad-band synchrotron radiation.

Assuming the spectrum of accelerated electrons is a power-law function with the index of p , and that a constant fraction ϵ_e of the shock energy is distributed to electrons, we could derive the minimum injected electron Lorentz factor as (for $p > 2$)

$$\gamma_m = \frac{p-2}{p-1} \epsilon_e (\gamma - 1) \frac{m_p}{m_e}, \quad (2)$$

where m_p and m_e are proton mass and electron mass respectively. Also assuming that a constant fraction ϵ_B of the shock energy density is distributed to the magnetic energy density behind the shock, one can obtain

$$B = (8\pi e \epsilon_B)^{1/2}, \quad (3)$$

where e is the energy density in the shocked region.

For synchrotron radiation, the observed radiation power and the characteristic frequency of an electron with Lorentz factor γ_e are given by (Rybicki and Lightman 1979)

$$P(\gamma_e) \simeq \frac{4}{3} \sigma_T c \gamma_e^2 \frac{B^2}{8\pi}, \quad (4)$$

$$\nu(\gamma_e) \simeq \gamma_e^2 \frac{q_e B}{2\pi m_e c}, \quad (5)$$

where the factors of γ^2 and γ are introduced to transform the results from the frame of the shocked fluid to the frame of the observer.

For an individual electron, the spectral power, P_ν (in unit of erg Hz $^{-1}$ s $^{-1}$) varies as $\nu^{1/3}$ for $\nu < \nu(\gamma_e)$, and cuts off exponentially for $\nu > \nu(\gamma_e)$ (Rybicki and Lightman 1979). The peak power occurs at $\nu(\gamma_e)$ with an approximate value of

$$P_{\nu,\text{max}} \approx \frac{P(\gamma_e)}{\nu(\gamma_e)} = \frac{m_e c^2 \sigma_T}{3q_e} \gamma B. \quad (6)$$

On the other hand, one could estimate the life time of a relativistic electron with Lorentz factor γ_e in the observer frame as

$$\tau(\gamma_e) = \frac{\gamma \gamma_e m_e c^2}{\frac{4}{3} \sigma_T c \gamma_e^2 \frac{B^2}{8\pi}} = \frac{6\pi m_e c}{\gamma \gamma_e \sigma_T B^2}. \quad (7)$$

By setting $\tau(\gamma_e) = t$, a critical electron Lorentz factor γ_c is defined,

$$\gamma_c = \frac{6\pi m_e c}{\gamma \sigma_T B^2 t}, \quad (8)$$

where t refers to the time in the observer frame. Above γ_c , synchrotron radiation cooling becomes significant, so that the electron distribution shape should be modified.

A third characteristic frequency ν_a , i.e., the synchrotron self-absorption frequency, could be defined by equating the synchrotron flux and the flux of a blackbody, i.e.

$$I_\nu^{\text{syn}}(\nu_a) = I_\nu^{\text{bb}}(\nu_a) \simeq 2kT \cdot \frac{\nu_a^2}{c^2} \quad (9)$$

where the blackbody temperature is

$$kT \simeq \max[\gamma_a, \min(\gamma_c, \gamma_m)] m_e c^2, \quad (10)$$

and γ_a is the corresponding electron Lorentz factor of ν_a for synchrotron radiation, i.e. $\gamma_a = (4\pi m_e c \nu_a / 3eB)^{1/2}$ (e.g. Sari & Piran 1999; Kobayashi & Zhang 2003).

In the Blandford-McKee regime, the characteristic synchrotron frequencies and the peak synchrotron flux density

$F_{\nu, \max} = 4\pi/3R^3 n P_{\nu, \max}$ for a constant circum-medium density could be expressed (Sari et al. 1998; Gao et al. 2013b).

$$\begin{aligned} \nu_m &= 8.1 \times 10^{11} \text{ Hz } (1+z)^{1/2} \left(\frac{p-2}{p-1} \right)^2 E_{52}^{1/2} \epsilon_{e,-1}^2 \epsilon_{B,-2}^{1/2} t_5^{-3/2}, \\ \nu_c &= 2.9 \times 10^{16} \text{ Hz } (1+z)^{-1/2} E_{52}^{-1/2} n_{0,0}^{-1} \epsilon_{B,-2}^{-3/2} t_5^{-1/2} \\ F_{\nu, \max} &= 1.1 \times 10^4 \mu\text{Jy } (1+z) E_{52} n_{0,0}^{1/2} \epsilon_{B,-2}^{-2} D_{28}^{-2}, \\ \nu_a &= 3.1 \times 10^9 \text{ Hz } (1+z)^{-6/5} \frac{g(p)}{g(3.2)} E_{52}^{1/5} n_{0,0}^{3/5} \epsilon_{e,-1}^{-1} \epsilon_{B,-2}^{1/5}, \end{aligned} \quad (11)$$

where $g(p) = \left(\frac{p-1}{p-2} \right) (p+1)^{3/5} \left(\frac{\Gamma(\frac{3p+22}{12}) \Gamma(\frac{3p+2}{12})}{\Gamma(\frac{3p+19}{12}) \Gamma(\frac{3p-1}{12})} \right)^{3/5}$ is a numerical constant relate to p .

Before applying the above DNS merger afterglow model to explain the PTF11agg data, we first simply summarize the observational properties of PTF11agg as follows (Cenko et al. 2013):

- Late time radio data suggest that the ejecta should be still relativistic even at a very late epoch;
- The optical light curve starts to decay at the very beginning of observation, i.e., $t_s = 2 \times 10^4$ s, with a simple power law decay slope $\alpha = 1.66 \pm 0.35$. The first optical flux in R band is about $180 \mu\text{Jy}$ (see Figure 1);
- The radio band (8 GHz) light curve reached its peak around 10^7 s, where the peak flux is about $200 \mu\text{Jy}$. The spectral slope for the early radio spectral regime is about $\beta = 1/3$ (until 5.8×10^6 s), implying that the radio peak should correspond to ν_m crossing.

First, to reach a relativistic speed for the ejecta, we need

$$M_{\text{ej}} \leq M_{\text{ej},c} \quad (12)$$

where $M_{\text{ej},c} \sim 6 \times 10^{-3} M_{\odot} I_{45} P_{0,-3}^{-2} \xi$ (defined by setting $E_{\text{rot}} \xi = 2(\gamma-1)M_{\text{ej},c,2} c^2$), above which the blast wave would never reach a relativistic speed (Gao et al. 2013a). Nevertheless, there is no obvious break for late radio light curve, implying that the ejecta is still in the relativistic regime (e.g. $\gamma-1 \geq 1$) until the end of the observation $t_e = 3 \times 10^7$ s. Since it is in the Blandford-McKee stage, the ejecta evolves as $\gamma \propto t^{-3/8}$, we thus have

$$\max(\gamma_{\text{sd}} - 1, \gamma_{\text{dec}} - 1) \geq \left(\frac{t_e}{t_s} \right)^{3/8}. \quad (13)$$

Second, since the R -band light curve starts to decay from the beginning of the observation, we thus have

$$\max(t_{\text{sd}}, t_{\text{dec}}) \leq t_s. \quad (14)$$

On the other hand, since the radio light curve (see Figure 1) implies that ν_m crosses the 8 GHz band at about $5.8 \times 10^6 \sim 1.2 \times 10^7$, we thus have

$$8.1 \times 10^{11} (1+z)^{1/2} \left(\frac{p-2}{p-1} \right)^2 E_{52}^{1/2} \epsilon_{e,-1}^2 \epsilon_{B,-2}^{1/2} \left(\frac{t_{\text{cross}}}{10^5} \right)^{-3/2} = 8 \times 10^9, \quad (15)$$

where

$$5.8 \times 10^6 < t_{\text{cross}} < 1.2 \times 10^7. \quad (16)$$

Moreover, from $\nu_m \propto t^{-3/2}$, one could easily estimate that $\nu_m(t_s) < \nu_{\text{opt}} = 5 \times 10^{14} \text{ Hz}$. We thus expect the optical band to fall into the spectrum regime $\nu_m < \nu_{\text{opt}} < \nu_c$. Consequently the observed temporal decay index ($\alpha_{\text{opt}} = 1.66 \pm 0.35$) can be translated directly into the electron spectral index p , i.e., for a constant-density medium as suggested by C13, we find $p = 3.2 \pm 0.47$. At t_s , we have

$$f_{\nu}(t_s) = F_{\nu, \max} \left(\frac{\nu}{\nu_m} \right)^{-1.1} \approx 180 \mu\text{Jy}. \quad (17)$$

Based on the peak flux in the radio band, we get

$$1.1 \times 10^4 (1+z) E_{52} n_{0,0}^{1/2} \epsilon_{B,-2}^{1/2} D_{28}^{-2} \approx 200 \quad (18)$$

Moreover, the self-absorption frequency should fall below the radio frequency range, i.e.,

$$3.1 \times 10^9 (1+z)^{-6/5} E_{52}^{1/5} n_{0,0}^{3/5} \epsilon_{e,-1}^{-1} \epsilon_{B,-2}^{1/5} < 8 \times 10^9. \quad (19)$$

Note that the ejecta formed in a DNS merger system would expand into a pulsar wind bubble created by the progenitor pulsars (Gallant & Achterberg 1999). The radius of the bubble could be about 10^{17} cm (Königl & Granot 2002). The value of ϵ_B should be relatively large in the bubble (Königl & Granot 2002). One can easily find that the optical signals of PTF11agg are emitted within this bubble radius (with ϵ_B), while the radio emission is emitted from outside (with $\tilde{\epsilon}_B = \eta \epsilon_B$, and $0 < \eta < 1$, see equations 15, 18 and 19).

From equations 12-14, we get the following constraints on the ejecta mass and spin down luminosity:

$$\begin{aligned} M_{\text{ej}} &\leq 1.1 \times 10^{-3} \xi M_{\odot} \\ L_{\text{sd},0} &\geq 1.5 \times 10^{48} \xi \text{ erg s}^{-1}. \end{aligned} \quad (20)$$

Combining equations 15-19, we have

$$\begin{aligned} \eta^{1/2} &= 0.006 \xi^{-1} (1+z)^{-1} n^{-1/2} \epsilon_{B,-2}^{-1/2} D_{28}^2 \\ n^{1/2} &= 0.93 \xi^{-1.55} (1+z)^{-1.55} \epsilon_{e,-1}^{-2.2} \epsilon_{B,-2}^{-1.05} D_{28}^2 \\ 1240 (1+z)^{-1.05} \xi^{-1.05} &\leq \epsilon_{e,-1}^{4.2} \epsilon_{B,-2}^{1.05} \leq 3921 (1+z)^{-1.05} \xi^{-1.05}. \end{aligned} \quad (21)$$

For a given redshift, we only get three independent constraints on five unknown parameters, i.e., ξ , n , ϵ_e , ϵ_B and η (note that $p = 3.2$ is fixed). This leaves us some degeneracy in choosing parameters to fit the data.

In the following, we fix $\xi = 1/3$ (i.e. $\sim 10^{52}$ erg spin down energy injected into the ejecta) and $\epsilon_e = 0.4$, and then fit the optical and radio data for different redshifts by adopting appropriate values for ϵ_B , n and η . One fitting result is shown in Figure 1, and the adopted parameters are collected in Table 1. With the chosen parameters, we have derived the corresponding X-ray flux, which is found to be consistent with the non-detection limitation.

In view of the fact that PTF11agg might be the first recognized candidate for DNS merger afterglow, it would be helpful to compare the inferred shock parameter values with those of other relativistic shock related phenomena, such as (15) GRBs. Recently, Santana et al. (2013) performed a careful literature search for ϵ_e and ϵ_B , and found that $\epsilon_e \sim 0.02 - 0.6$ and $\epsilon_B \sim 3.5 \times 10^{-5} - 0.33$ were favored by the observations. With GRB optical afterglow data, Liang et al. (2013) found

TABLE 1
ADOPT PARAMETERS FOR FITTING THE OPTICAL AND RADIO DATA OF
PTF11AGG FOR DIFFERENT REDSHIFT.

z	n (cm^{-3})	ϵ_e	ϵ_B	η	ξ	p
0.5	1.0×10^{-4}	0.4	0.08	0.09	0.3	3.2
1	2.4×10^{-3}	0.4	0.06	0.09	0.3	3.2
3	0.26	0.4	0.03	0.09	0.3	3.2

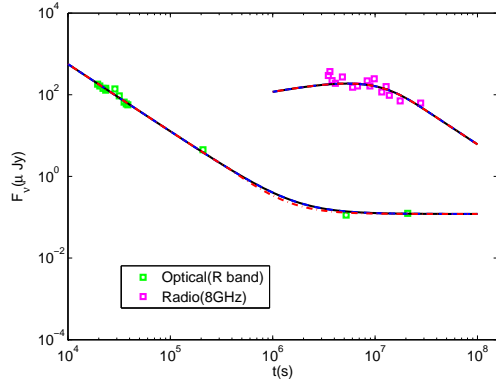


FIG. 1.— Optical and radio (8 GHz) light curves for PTF11agg, with best fittings by assuming different redshift for the source. The green square denotes the optical observation and the purple squares denote the radio data. The black solid line is for $z = 0.5$, the blue dash line is for $z = 1$ and the red dash-dot line is for $z = 3$.

that the electron spectral index p is distributed in the range from 2 to 3.5¹. Moreover, Shen et al. (2006) performed a general investigation for relativistic sources, such as GRBs (with both prompt and afterglow data), blazars and pulsar wind nebulae, and found a similar broad distribution of p . Our inferred parameters from the DNS merger afterglow model fall well within the ranges of these parameter distributions.

4. DISCUSSION

We have proposed a DNS merger origin for the cosmological relativistic fading source PTF11agg. Based on the observational properties of PTF11agg, we analytically constrained the parameter space for the DNS merger afterglow model and then fit the multi-band data by adopting appropriate parameter values. We find that the DNS merger afterglow model could fit both the optical and radio data well regardless of the source redshift. If our interpretation is correct, the following implications can be inferred:

First, the next generation gravitational-wave (GW) detectors are expected to detect GW signals from mergers of two compact objects, with DNS mergers as primary targets. PTF11agg-like transients could be potential electromagnetic counterparts to such GW signals. The study of PTF11agg-like transients would not only shed light on the nature of the DNS merger scenario itself, but also contribute to identifying the astrophysical origin of GW signals.

Second, since DNS mergers are proposed to be the progenitor of short GRBs, the lack of a high energy counterpart for PTF11agg could be due to the fact that our line of sight is not along the direction of the jet axis. If so, there exists the possibility of simultaneously detecting a short GRB afterglow and

(off-beam) PTF11agg-like emission, when our line of sight is within the jet opening angle. Since the PTF11agg-like emission component is Doppler de-boosted with respect to the on-beam calculations (Gao et al. 2013a), it is detectable only under favorable condition. Some short GRB afterglow features may be accounted for within this picture (H. Gao et al. 2013, in preparation).

Third, besides the bright afterglow discussed by Gao et al. (2013a) and this Letter, the DNS merger scenario with a supra-massive central engine was also proposed to give rise to other bright electromagnetic counterparts: the dissipation of a Poynting flux dominated outflow from proto-magnetar would power a bright early X-ray afterglow (Zhang 2013); the magnetar wind would add energy to the ejecta, giving rise to a brighter “merger-nova” than the pure r -process powered one (Yu et al. 2013; Metzger & Piro 2013); Recently the short GRB 130603B has attracted attention by showing an infrared excess in its late emission (Tanvir et al. 2013; Berger et al. 2013). Even though it was suggested that this emission is consistent with the r -process powered “kilonova” emission with a black hole central engine, some authors have already pointed out that both the mergernova and short GRB afterglow of this burst can be understood within the scenario of a supra-massive magnetar central engine, as long as a large fraction of magnetar spin-energy is lost, possibly by GW radiation (Fan et al. 2013; Metzger & Piro 2013). If so, the short-lived transient emission from GRB 130603B and PTF11agg may be different manifestations of the same intrinsic phenomenon with different viewing angles and/or magnetar parameters.

Finally, due to the large uncertainty of the DNS merger event rate and the fraction of mergers that produce stable magnetars, it is difficult to predict the detection rate by blind surveys for DNS merger afterglows (e.g. Yu et al. 2013, for a discussion). C13 suggested the event rate of PTF11agg-like sources is ~ 5 times that of normal GRBs, namely $5 \text{ Gpc}^{-3} \text{ yr}^{-1}$. Assuming a fraction f of DNS mergers may give rise to PTF11agg-like events, one can estimate the DNS merger events rate as $\mathcal{N} \sim 5/f \text{ Gpc}^{-3} \text{ yr}^{-1} = 50f_{-1}^{-1} \text{ Gpc}^{-3} \text{ yr}^{-1}$ (Gao et al. 2013c), which is consistent with predictions using other methods (Phinney 1991; Kalogera et al. 2004; Abadie et al. 2010).

We note that Wang & Dai (2013) also proposed a different model for PTF11agg within the same framework as this Letter. They assumed that the magnetar wind injection is in the form of electron/positron pairs rather than a Poynting flux, and they interpreted the observed emission from the reverse shock region. They obtained different model parameter values and different spectral properties from ours. Future observations with a larger sample of PTF11agg-like transients may be helpful to distinguish between these two models, and consequently lead to a diagnosis of the composition of the magnetar wind.

We acknowledge the National Basic Research Program (“973” Program) of China under Grant No. 2014CB845800, 2013CB834900 and 2009CB824800. This work is also supported by the National Natural Science Foundation of China (grant No. 11033002 & 10921063). XFW acknowledges support by the One-Hundred-Talents Program and the Youth Innovation Promotion Association of Chinese Academy of Sciences.

¹ Note that medium density profile is relevant for determining the electron index p . For a general circumburst medium density profile $n \propto r^{-k}$ as adopted in Liang et al. (2013), the derived p would be somewhat larger than the value

derived by assuming a constant density of the medium

REFERENCES

- Abadie, J., Abbott, B. P., Abbott, R., et al. 2010, *Classical and Quantum Gravity*, 27, 173001
- Barthelmy, S. D., Barbier, L. M., Cummings, J. R., et al. 2005, *Space Sci. Rev.*, 120, 143
- Berger, E., Fong, W., Chornock, R. 2013, *ApJ*, 774, L23
- Blandford, R. D., & McKee, C. F. 1976, *Physics of Fluids*, 19, 1130
- Bloom, J. S., Giannios, D., Metzger, B. D., et al. 2011, *Science*, 333, 203
- Burrows, D. N., Hill, J. E., Nousek, J. A., et al. 2005, *Space Sci. Rev.*, 120, 165
- Burrows, D. N., Kennea, J. A., Ghisellini, G., et al. 2011, *Nature*, 476, 421
- Cenko, S. B., Krimm, H. A., Horesh, A., et al. 2012, *ApJ*, 753, 77
- Cenko, S. B., Kulkarni, S. R., Horesh, A., et al. 2013, *ApJ*, 769, 130
- Dai, Z. G., & Lu, T. 1998a, *A&A*, 333, L87
- Dai, Z. G., & Lu, T. 1998b, *PRL*, 81, 4301
- Dai, Z. G., Wang, X. Y., Wu, X. F., & Zhang, B. 2006, *Science*, 311, 1127
- Fan, Y. Z., Yu, Y. W., Xu, D., et al. 2013, *ApJL*, in press
- Gallant, Y. A., & Achterberg, A. 1999, *MNRAS*, 305, L6
- Gao, H., Ding, X., Wu, X.-F., Zhang, B., & Dai, Z.-G. 2013a, *ApJ*, 771, 86
- Gao, H., Lei, W.-H., Zou, Y.-C., Wu, X.-F., Zhang, B., 2013b, *New Astronomy Review*, 57, 141
- Gao, H., Zhang, B., Wu, X.-F., & Dai, Z.-G. 2013c, *Phys. Rev. D*, 88, 043010
- Gehrels, N., & Razzaque, S. 2013, *Frontiers of Physics*, 2
- Ghisellini, G., Padovani, P., Celotti, A., & Maraschi, L. 1993, *ApJ*, 407, 65
- Giacomazzo, B., & Perna, R. 2013, *ApJ*, 771, L26
- Hurley, K., Golenetskii, S., Aptekar, R., et al. 2010, in *Deciphering the Ancient Universe with Gamma-Ray Bursts*, Vol. 1279, American Institute of Physics Conference Series, ed. N. Kawai & S. Nagataki, 330
- Hotokezaka, K., Kiuchi, K., Kyutoku, K., et al. 2013, *Phys. Rev. D*, 87, 024001
- Kalogera, V., Kim, C., Lorimer, D. R., et al. 2004, *ApJ*, 601, L179
- Kobayashi, S., Zhang, B., 2003, *ApJ*582, L75
- Königl, A., & Granot, J. 2002, *ApJ*, 574, 134
- Krawczynski, H., & Treister, E. 2013, *Frontiers of Physics*, 26
- Lei, W.-H., & Zhang, B. 2011, *ApJ*, 740, L27
- Lei, W.-H., Zhang, B., & Gao, H. 2013, *ApJ*, 762, 98
- Liang, E., Li, L., Gao, H., et al. 2013, *ApJ*, 774, 13
- Meegan, C., Lichti, G., Bhat, P. N., et al. 2009, *ApJ*, 702, 791
- Mészáros, P. 2006, *Reports on Progress in Physics*, 69, 2259
- Metzger, B. D., & Piro, A. L. 2013, arXiv:1311.1519
- Nakar, E., Piran, T., & Granot, J. 2002, *ApJ*, 579, 699
- Perley, R. A., Chandler, C. J., Butler, B. J., & Wrobel, J. M. 2011, *ApJ*, 739, L1
- Rezzolla, L., Giacomazzo, B., Baiotti, L., et al. 2011, *ApJ*, 732, L6
- Phinney, E. S. 1991, *ApJ*, 380, L17
- Rhoads, J. E. 1997, *ApJ*, 487, L1
- Rosswog, S., Piran, T., & Nakar, E. 2013, *MNRAS*, 430, 2585
- Rybicki, G. B., Lightman, A. P., 1979. *Radiative processes in astrophysics*. New York, Wiley-Interscience, 1979. 393 p.
- Santana, R., Barniol Duran, R., & Kumar, P. 2013, arXiv:1309.3277
- Sari, R., Piran, T., & Narayan, R. 1998, *ApJ*, 497, L17
- Sari, R., Piran, T., 1999, *ApJ*, 529, 541
- Shen, R., Kumar, P., & Robinson, E. L. 2006, *MNRAS*, 371, 1441
- Soderberg, A. M., Chakraborti, S., Pignata, G., et al. 2010, *Nature*, 463, 513
- Tanvir, N. R. et al. 2013, *Nature*, 500, 547
- Wang, L.-J., & Dai, Z.-G. 2013, *ApJ*, 774, L33
- Yu, Y.-W., Zhang, B., & Gao, H. 2013, *ApJ*, 776, L40
- Zhang, B., Mészáros, P. 2001, *ApJ*, 552, L35
- Zhang, B., & Mészáros, P. 2004, *International Journal of Modern Physics A*, 19, 2385
- Zhang, B. 2013, *ApJ*, 763, L22